Modal Decomposition on Sound Propagation in Ducts with and without Flow

João Luís Aguiar Oliveira Rosa

joao.aguiar@ist.utl.pt

Técnico Lisboa
Lisbon, Portugal

September 10, 2014

Abstract

Methodologies outlined for the study of two-port acoustic sources allowed the characterization of the modal scattering matrix for different obstacles and duct terminations with the determination of transmission and reflection coefficients with and without in-duct flow.

It was concluded that flow alters reflection mechanisms at duct terminations, decreasing direct reflections and increasing convertive reflections both upstream and downstream. For two-port sources flow increased transmission factors on the upstream side at the same time it decreased reflections downstream. Active part measurements allowed to identify how a diaphragm in the presence of flow generates flow-induced noise. Spinning induced flow favored upstream transmission factors for modes with the same spinning direction of the fan and suppressed its downstream counterparts.

There is not, to the author's knowledge, any record of such complex spectral modal decomposition computations for two-port sources prior to those performed in the IDEALVENT context and described in the present thesis.

1 Introduction

Every day millions of passengers travel on airliners, usually unaware of the complex Environmental Control Systems (ECS) that guarantee them healthy conditions inside the aircraft cabins they're traveling in and prevents them from the effects of the lower pressures at the altitudes planes fly.

ECS systems rely on a panoply of ducts and fans to provide passengers and crew with renovated, clean air at the same time they cope with outside altitude variations by pumping more air into the cabin in order to stabilize cabin pressure. These equipments of course generate noise (being key contributors to the acoustic nuisance not only within the cabin but also around grounded aircraft). Since reaching low levels of cabin and ramp noise is crucial not only to ensure the satisfaction of aircraft passengers but also a safe working environment for the crew this has become an important research subject in aeroacoustics.

ECS noise reduction constitutes the leitmotif for an insight into duct acoustics since this is a mostly common situation regarding ECS, where so much of the installations comprises exactly of all sorts of ducts.

2 Duct Acoustics: Theoretical Background

If the duct domain is simplified by a general cylindrical volume it has been shown that the sound field inside the duct can be given by the sum of Bessel Functions, with each function being related to one propagation mode. In cylindrical coordinates the expression comes as follows:

$$p\prime(x,r,\theta) = \sum_{m=-\infty}^{\infty}\sum_{n=0}^{\infty}\left(p^{+}_{m,n}\mathrm{e}^{-ik^{+}_{m,n}x} + p^{-}_{m,n}\mathrm{e}^{+ik^{-}_{m,n}x}\right) f_{m,n}(r)\mathrm{e}^{im\theta} \tag{1}$$

This sound field expression takes into account all the coordinates (x,r and θ). By changing these factors and assuming the sum of all modes in presence it is possible to predict the acoustic pressure of both moving directions at any given position.

$p^{\pm}_{m,n}$ represents the acoustic pressure of both directions inside the duct (plus and minus amounting to left and right moving). The exponential terms including $\pm ik^{+}_{m,n}x$ are relative to the axial position along the duct with $k^{\pm}$ being the wave number relative to the waves propagation along x (the duct's axis of symmetry) and so designated by axial wave number [1]

$$k^{\pm}_{mn} = \frac{w}{c_0}\frac{\sqrt{1-\left(\frac{\alpha_{mn}}{R}\frac{c_0}{w}\right)^2(1-M^2)}\mp M}{1-M^2} \tag{2}$$

Where R is the duct's inner radius, c_0 the speed of sound, M the Mach number, and α is the "n^{th} nonnegative zero of J'_m" [2] (J'_m is the second derivative of the Bessel Function of order m) .

The term $\mathrm{e}^{im\theta}$ regards the point's azimuthal position in the plane and is associated with m which, by extension, is designated by azimuthal wave number.

Finally $f_{m,n}(r)$ takes into account the point's position along the duct's inner radius (i.e. closer or further away from the plane section's center) and is given by

$$f_{m,n}(r) = \frac{J_m(\alpha_{mn}r/R)}{\sqrt{N_{m,n}}} \tag{3}$$

Where in the normalization $\sqrt{N_{m,n}}$ the expression $N_{m,n}$ is given by ([11])

$$N_{mn} = J^2_m(\alpha_{mn}) - J_{m-1}(\alpha_{mn})\,J_{m+1}(\alpha_{mn}) \tag{4}$$

2.1 Modes and Cut-off frequencies

If we consider the formulation for the axial wave number k_{mn} given in eq. 2 it comes as a consequence that should the value of k_{mn} be complex its product by the complex number i would mean that the axial term would have a negative exponent in eq. 1.

Such a mode would then propagate with decreasing amplitude given the term $\mathrm{e}^{-\alpha x}$, which means it would be evanescent, or *cut off*. In the same way, modes with real k_{mn} are considered to propagate, and so are called *cut on*.

It is important then to find the frequencies for which k_{mn} becomes real or complex. Let's go back to eq. 2, but this time taking into account only the expression inside the square root. It is known that k_{mn} will have a complex value when the term inside the square root is negative. Therefore we can get the values of w (and from these, the frequencies) with which k_{mn} acquires either real or complex values:

$$f_{cut-on_{mn}} = \frac{\alpha_{mn}\cdot c_0}{2\pi R}\frac{1}{\sqrt{1-M^2}} \tag{5}$$

Since equation 1 already includes all modes it means we can describe the sound field using not the sum of all possible modes, but the *sum of all propagating modes*, whose k_{mn} is real.

Because *"the zeros of J'_m form an ever increasing sequence both in m and in n [...] there are for any w always a $m = m_0$ and $n = n_0$ beyond which [...] k_{nm} is purely imaginary, and the mode decays exponentially in x"* [2], it means that for increasing frequencies the value of α_{mn} we will also have to increase for the cut-on condition to be met and so higher order modes will require higher frequencies being emitted.

Modes follow therefore the order of their eigenvalues [19]. The first three modes are shown below, together with the sixth propagation mode. However, since the sixth eigenvalue corresponds in fact to $m = n = 1$ it means that the sixth mode has $\alpha_{mn} = \alpha_{11} = 5.331$. Hence such mode will have characteristics of the first radial and the first azimuthal modes. It is called an hybrid mode.

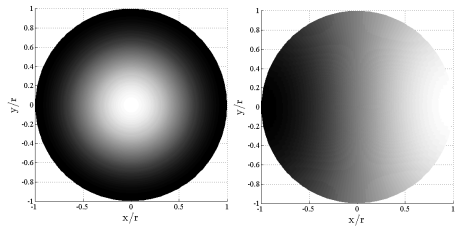

Figure 1: 1^{st} and 2^{nd} azimuthal propagation modes, $(m = 1, n = 0)$ and $(m = 2, n = 0)$

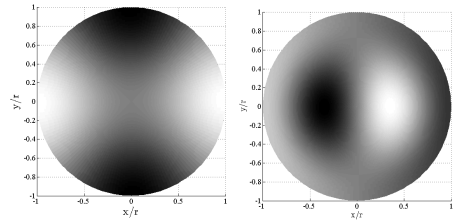

Figure 2: 3^{rd} azimuthal mode and the first hybrid mode, $(m = 3, n = 0)$ and $(m = 1, n = 1)$

3 Experimental Methodology

3.1 The Two-Microphone Method: Terminations

The two-microphone method has been in use for decades in the study of duct acoustics. The process, based on the solving of the sound field at two given positions inside the ducts, allows the researcher to obtain the acoustic pressure of both left and right moving waves within the plane wave region (all frequencies below the first cut-on frequency).

The method can be understood if we begin by taking eq. 1 and make $m = n = 0$. By this we are only admitting the terms relative to the plane wave, and eq. 1 simplifies into

$$p\prime(x, r, \theta) = \left(p^{+}_{0,0}\mathrm{e}^{-ik^{+}_{0,0}x} + p^{-}_{0,0}\mathrm{e}^{+ik^{-}_{0,0}x}\right) f_{0,0}(r)\mathrm{e}^{i0\theta} \tag{6}$$

For a simpler notation we'll make $p^{\pm}_{0,0} \coloneqq p^{\pm}_{0,0} \cdot f(r)$:

$$p\prime(x, r, \theta) = p^{+}\mathrm{e}^{-ik^{+}x} + p^{-}\mathrm{e}^{+ik^{-}x} \tag{7}$$

with the first term referring to the wave propagating in the positive direction and the second to the one propagating in the opposite direction (see fig. 3).

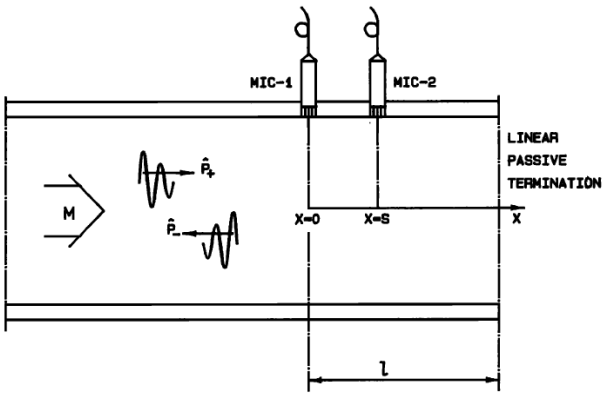

Figure 3: Schematic view of left and right moving waves in the plane wave region [3]

If we define the reflection coefficient as the ratio between emitted and reflected wave amplitudes this means that to compute the reflection coefficient at duct's termination on the right:

$$R = \frac{p^{-}}{p^{+}} \tag{8}$$

Microphones are not able to distinguish left moving from right moving waves, since they measure only the "overall" pressure $p\prime$. If we measure the acoustic field at two given points (A and B, respectively) separated by a distance s (see fig. 3) and solve the following system of equations (p^{+} and p^{-} are the same for both A and B)

$$p\prime_A = p^{+}\mathrm{e}^{-ik^{+}x_A} + p^{-}\mathrm{e}^{+ik^{-}x_A} \tag{9a}$$

$$p\prime_B = p^{+}\mathrm{e}^{-ik^{+}x_B} + p^{-}\mathrm{e}^{+ik^{-}x_B} \tag{9b}$$

The following expression for the plane wave reflection coefficient is obtained

$$R = \frac{p^{-}}{p^{+}} = \frac{\dfrac{1}{\mathrm{e}^{ik^{-}_s} - \mathrm{e}^{-ik^{+}_s}}\left(p\prime_B - p\prime_A\mathrm{e}^{-ik^{+}_s}\right)}{\dfrac{1}{\mathrm{e}^{ik^{-}_s} - \mathrm{e}^{-ik^{+}_s}}\left(p\prime_A\mathrm{e}^{ik^{-}_s} - p\prime_B\right)} \tag{10}$$

3.2 The Two-Microphone Method Two-Ports

When instead of a termination we intend to study a two-port a coupling between the inlet and outlet is present and conditions on both sides (inlet and outlet) may change. We can no longer study only one side (inlet or outlet) and are in fact forced to "duplicate" the analysis performed in the previous section in order to study both ports.

For this it is wise to consider a configuration similar to that represented in fig. 4:

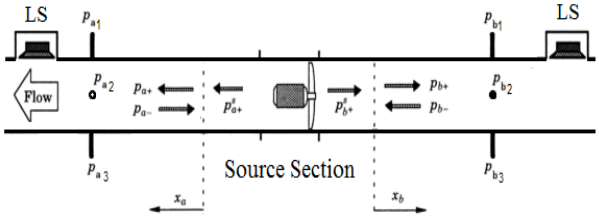

Figure 4: Microphone set for the study of an acoustic two-port source [4]

The relation between $p_a^{\pm}$ and $p_b^{\pm}$ can be summarized by computing the transmission and reflection coefficients and adding the source generated acoustic pressure p^s. This can be rationalized in the following way: for each side of the two-port the "outwards moving" wave (identified by a "+" sign) will be given by the sum of the source generated sound, the transmitted sound from the opposing port, and the reflected sound at the port we are analyzing. For side a this is equivalent to the expression

$$p_a^+ = \overbrace{\rho_a \cdot p_a^-}^{\text{reflection at } a} + \overbrace{\tau_b \cdot p_b^-}^{\text{transmission across } b} + \overbrace{p_a^{s+}}^{\text{source sound at } a} \tag{11}$$

Where ρ_a represents the reflection coefficient at ports a and b, τ_a the transmission coefficient across the two-port source from b to a, and $p_a^{\pm}$ the source generated sound at a moving in the left-to-right direction. If we expand this for the entire two port we get, in the matrix form, for both ports a and b:

$$\begin{bmatrix} p_a^+ \\ p_b^+ \end{bmatrix} = \begin{bmatrix} \rho_a & \tau_b \\ \tau_a & \rho_b \end{bmatrix} \begin{bmatrix} p_a^- \\ p_b^- \end{bmatrix} + \begin{bmatrix} p_a^{s+} \\ p_b^{s+} \end{bmatrix} \equiv p^+ = Sp^- + p^s \tag{12}$$

Here an important step is taken: if we assume that in the presence of two external loudspeakers located respectively upstream and downstream from the two-port source the sound by them generated dominates over the sound field generated by the two-port source we can then evaluate eq. 12 ignoring the source generated sound (making $p^s = 0$) and therefore studying the two-port's passive part with eq. 13:

$$\begin{bmatrix} p_a^+ \\ p_b^+ \end{bmatrix} = \begin{bmatrix} \rho_a & \tau_b \\ \tau_a & \rho_a \end{bmatrix} \begin{bmatrix} p_a^- \\ p_b^- \end{bmatrix} \tag{13}$$

Where if we consider the two-microphone method already analyzed in section 3.1 to be applied on both ends of the two-port to provide us with $p_a^{\pm}$ and $p_b^{\pm}$ we can obtain the "transfer matrix" S, whose components correspond to the transmission and reflection coefficients of the two-port source. By testing the system with two different states (here denoted in roman notation I and II) both upstream and downstream (that is, with one loudspeaker downstream and another upstream) we will therefore have two more state equations to solve, since we have expanded both p^+ and p^- from 2×1 vectors to 2×2 matrices. Which now allows us to easily compute the scattering matrix by doing

$$S = \begin{bmatrix} p_a^{+I} & p_a^{+II} \\ p_b^{+I} & p_b^{+II} \end{bmatrix} \cdot \begin{bmatrix} p_a^{-I} & p_a^{-II} \\ p_b^{-I} & p_b^{-II} \end{bmatrix}^{-1} \tag{14}$$

After computing the scattering matrix of the two-port source the next logical step is therefore to compute p^s which represents, as referred before, the sound generated by the two-port source while working. Be it a fan, a pump, or any other ECS component.

Returning to the main equation in two-port analysis:

$$p^+ = Sp^- + p^s \tag{15}$$

Although it can be taken straightforwardly that the source generated acoustic pressure is given by $p^s = p^+ - Sp^-$ it is wise to represent p^s in order to the acoustic pressures measured at a and b by doing $p^s = Cp$, where p is

a vector composed of the acoustic pressures registered at each first microphone on each side of the two-port and C is in fact a function of the scattering matrix:

$$\begin{bmatrix} p_a^{s+} \\ p_b^{s+} \end{bmatrix} = [C] \begin{bmatrix} p_{a1} \\ p_{b1} \end{bmatrix} \tag{16}$$

Where C is the simplification of the passive-part process and the solving of eq.15:

$$C = (I - SR)(I + R)^{-1} \tag{17}$$

With I being the identity matrix and R the reflection matrix of the two-port sides. At first the computation of R may seem tricky, since it can easily be mistaken by matrices $\rho_{a/b}$. Here one should stop and take time to understand what is actually the difference between $R_{a/b}$ and $\rho_{a/b}$: whereas $\rho_{a/b}$ represents the reflection at the two-port side $R_{a/b}$ refers to the reflection at the microphone section, obtained by measuring the sound field at $a1$ and $b1$ and given by the very same procedure that allowed us to compute the reflection coefficient on the previous section.

3.3 Expanding the Two-Microphone Method

3.3.1 Terminations

Since it was the objective of this research to perform a modal decomposition analysis it became necessary to expand the two-microphone method in order to include other modes than the plane wave. For this the two-microphone set was substituted by a sixteen microphone set as shown in fig. 5

If we repeat the procedure from sec. 3.1, but this time including more modes in the sound field expressions for both microphones it becomes evident that this time we have not only two unknowns, which means that the expanded microphone method for the study of plane wave together with the first azimuthal mode will therefore require the measuring of the sound field at six different positions (see eqs. below):

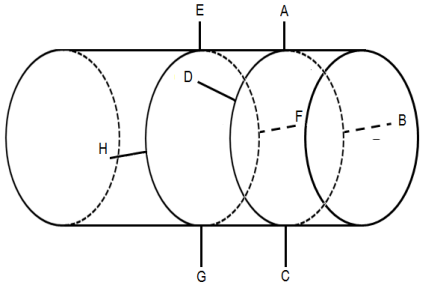

Figure 5: Schematic view of an expanded analysis microphone set

$$\begin{aligned} &p\prime_A : \\ &\left(p^+_{-N,0}\mathrm{e}^{-ik^+_{-N,0}x_A} + p^-_{-N,0}\mathrm{e}^{+ik^-_{-N,0}x_A}\right) f_{-N,0}(r_A)\mathrm{e}^{im\theta_A} + \\ &\qquad \cdots \\ &+\left(p^+_{+N,0}\mathrm{e}^{-ik^+_{+N,0}x_A} + p^-_{+N,0}\mathrm{e}^{+ik^-_{+N,0}x_A}\right) f_{+N,0}(r_A)\mathrm{e}^{im\theta_A} \end{aligned} \tag{18a}$$

$$\begin{aligned} &p\prime_B : \\ &\left(p^+_{-N,0}\mathrm{e}^{-ik^+_{-N,0}x_B} + p^-_{-N,0}\mathrm{e}^{+ik^-_{-N,0}x_B}\right) f_{-N,0}(r_B)\mathrm{e}^{im\theta_B} + \\ &\qquad \cdots \\ &+\left(p^+_{+N,0}\mathrm{e}^{-ik^+_{+N,0}x_B} + p^-_{+N,0}\mathrm{e}^{+ik^-_{+N,0}x_B}\right) f_{+N,0}(r_B)\mathrm{e}^{im\theta_B} \end{aligned} \tag{18b}$$

At this point it is worth to represent each sound field equation in a matricial form, since the notation used so far would prove too complex when the time came to express $p^{\pm}_{-N\cdots+N,N_R}$ in order to $p\prime_{A\cdots F}$. We will then link partial pressures $p^{\pm}$ with the terms related only to microphones position and wave's axial wave number in the following way (N represents the higher order azimuthal mode in

study and N_R the highest radial mode in study):

$$\begin{bmatrix} p\prime_A \\ \vdots \\ p\prime_N \end{bmatrix} = J \begin{bmatrix} p^+_{-N,0} \\ p^-_{-N,0} \\ p^+_{0,0} \\ p^-_{0,0} \\ p^+_{+N,0} \\ p^-_{+N,0} \\ p^+_{+N,N_R} \\ p^-_{+N,N_R} \end{bmatrix} \tag{19}$$

With J being given by

$$J = \begin{bmatrix} \mathrm{e}^{-ik^+_{-N,0}x_A} f_{-N,0}(r_A)\mathrm{e}^{iN\theta_A} & \cdots & \mathrm{e}^{+ik^-_{N,0}x_A} f_{N,0}(r_A)\mathrm{e}^{iN\theta_A} \\ \vdots & \cdots & \vdots \\ \vdots & \cdots & \vdots \\ \mathrm{e}^{-ik^+_{-N,0}x_F} f_{-N,0}(r_F)\mathrm{e}^{iN\theta_F} & \cdots & \mathrm{e}^{+ik^-_{N,0}x_F} f_{N,0}(r_F)\mathrm{e}^{iN\theta_F} \end{bmatrix} \tag{20}$$

From here we pass on to the following task of computing the reflection coefficients at the termination in analysis. Notice we can no longer speak of "a reflection coefficient" since now we have more modes in presence, each one with its own reflection coefficient, and, as we'll later see, interacting with other modes.

This said, we'll analyze the reflection mechanism in the following way, as done before, but this time instead of a fraction the multiplication of both matrices [5]

$$[R] = \left[p^-\right] \cdot \left[p^+\right]^{-1} \tag{21}$$

Where p^- and p^+ are column vectors whose components are the left and right moving modal waves for several different states in order to make sure the matrices can be inverted:

$$p^{\pm} = \begin{bmatrix} {p^{\pm}_{-N,0}}^{I} & \cdots & \cdots & {p^{\pm}_{-N,0}}^{2N+1} \\ \vdots & \cdots & \cdots & \vdots \\ {p^{\pm}_{+N,0}}^{I} & \cdots & \cdots & {p^{\pm}_{+N,0}}^{2N+1} \\ {p^{\pm}_{+N,N_R}}^{I} & \cdots & \cdots & {p^{\pm}_{+N,N_R}}^{2N+1} \end{bmatrix} \tag{22}$$

Which in turn yields the reflection matrix at the termination:

$$R = \begin{bmatrix} R_{-N,0} & \cdots & \cdots & \cdots & R_{-N,0} \\ \vdots & \ddots & \cdots & \cdots & \vdots \\ R_{0,0} & \cdots & R_{0,0} & \cdots & R_{0,0} \\ \vdots & \cdots & \cdots & \ddots & \vdots \\ R_{N,0} & \cdots & \cdots & \cdots & R_{N,0} \\ R_{N,N_R} & \cdots & \cdots & \cdots & R_{N,N_R} \end{bmatrix} \tag{23}$$

It is possible to understand that terms in the diagonal represent direct reflections (modes being reflected as themselves) while the remainder refer to convertive reflections (modes being reflected as different modes).

3.3.2 Two-ports

The methodology required for the modal decomposition of sound being produced and generated in two-port sources follows the same procedure as was shown for the expanded analysis in terminations. As we have seen p^+ and p^- are no longer single values, but column vectors with pressure coefficients for each mode and direction. We can then perform such a substitution in eq. 15 to calculate the source's passive part:

$$S = \begin{bmatrix} {p^+_{a_{-N,0}}}^{I} & \cdots & {p^+_{a_{-N,0}}}^{VI} \\ {p^+_{a_{0,0}}}^{I} & \cdots & {p^+_{a_{0,0}}}^{VI} \\ {p^+_{a_{+N,0}}}^{I} & \cdots & {p^+_{a_{+N,0}}}^{VI} \\ {p^+_{a_{-N\cdots+N,N_R}}}^{I} & \cdots & {p^+_{a_{+N,N_R}}}^{VI} \\ {p^+_{b_{-N,0}}}^{I} & \cdots & {p^+_{b_{-N,0}}}^{VI} \\ {p^+_{b_{0,0}}}^{I} & \cdots & {p^+_{b_{0,0}}}^{VI} \\ {p^+_{b_{+N,0}}}^{I} & \cdots & {p^+_{b_{+N,0}}}^{VI} \\ {p^+_{b_{-N\cdots+N,N_R}}}^{I} & \cdots & {p^+_{b_{+N,N_R}}}^{VI} \end{bmatrix} \cdot \begin{bmatrix} {p^-_{a_{-N,0}}}^{I} & \cdots & {p^-_{a_{-N,0}}}^{VI} \\ {p^-_{a_{0,0}}}^{I} & \cdots & {p^-_{a_{0,0}}}^{VI} \\ {p^-_{a_{+N,0}}}^{I} & \cdots & {p^-_{a_{+N,0}}}^{VI} \\ {p^-_{a_{-N\cdots+N,N_R}}}^{I} & \cdots & {p^-_{a_{+N,N_R}}}^{VI} \\ {p^-_{b_{-N,0}}}^{I} & \cdots & {p^-_{b_{-N,0}}}^{VI} \\ {p^-_{b_{0,0}}}^{I} & \cdots & {p^-_{b_{0,0}}}^{VI} \\ {p^-_{b_{+N,0}}}^{I} & \cdots & {p^-_{b_{+N,0}}}^{VI} \\ {p^-_{b_{-N\cdots+N,N_R}}}^{I} & \cdots & {p^-_{b_{+N,N_R}}}^{VI} \end{bmatrix}^{-1} \tag{24}$$

With the transfer matrix S now being given by (notice how reflection and transmission terms are now matrices themselves):

$$S = \begin{bmatrix} \begin{bmatrix} \rho_a \\ \tau_a \end{bmatrix} & \begin{bmatrix} \tau_b \\ \rho_b \end{bmatrix} \end{bmatrix} \tag{25}$$

In the expanded form:

$$S = \begin{bmatrix} \begin{bmatrix} \rho_{a\,-N,0} & \cdots & \cdots \\ \cdots & \rho_{a\,0,0} & \cdots \\ \cdots & \cdots & \rho_{a\,+N,+N} \\ \rho_{a\,N,N_R} & \cdots & \rho_{a\,N,N_R} \end{bmatrix} & \begin{bmatrix} \tau_{b\,-N,0} & \cdots & \cdots \\ \cdots & \tau_{b\,0,0} & \cdots \\ \cdots & \cdots & \tau_{b\,+N,+N} \\ \tau_{b\,N,N_R} & \cdots & \tau_{b\,N,N_R} \end{bmatrix} \\ \begin{bmatrix} \tau_{a\,-N,0} & \cdots & \cdots \\ \cdots & \tau_{a\,0,0} & \cdots \\ \cdots & \cdots & \tau_{a\,+N,+N} \\ \tau_{a\,N,N_R} & \cdots & \tau_{a\,N,N_R} \end{bmatrix} & \begin{bmatrix} \rho_{b\,-N,0} & \cdots & \cdots \\ \cdots & \rho_{b\,0,0} & \cdots \\ \cdots & \cdots & \rho_{b\,+N,+N} \\ \rho_{b\,N,N_R} & \cdots & \rho_{b\,N,N_R} \end{bmatrix} \end{bmatrix} \tag{26}$$

Matrices τ_a and τ_b describe the transmission process across the two-port with some modes being transmitted as themselves (propagating through the source without suffering scattering) and others being converted into different propagation modes. ρ_a and ρ_b represent the reflection coefficients on both sides of the two-port source.

The active part of the two-port source is calculated in the same way as before, with terms being expanded to take into account the different propagating modes.

$$\begin{bmatrix} p_a^{s+} \\ p_b^{s+} \end{bmatrix} = \begin{bmatrix} C \end{bmatrix} \begin{bmatrix} p_{a1} \\ p_{b1} \end{bmatrix} \tag{27}$$

Where C is now given by

$$C = (I - SR)\,(I + R)^{-1} \tag{28}$$

From here we obtain for R from the exact same equation we used previously:

$$R = \left[p^-\right] \cdot \left[p^+\right]^{-1} \tag{29}$$

This allows us then to compute C and solve eq. 27.

As a final remark one should notice that in the same way we have decomposed the external source generated sound so far we will also also a $(2N+1+N_R)\times 1$ vector for p^s, with each term representing the acoustic pressure emitted in each mode.

3.4 Experimental Over-Determination

If we think of two-port analysis or even a termination study we realize that most of possible errors come from flow induced noise. On cannot, in fact, neglect the turbulence effects in microphones since it induces a disturbance in measurements mostly impossible to predict and difficult to cope with.

It has been shown [1, 6] that by assembling measurements by more than $2N+1$ loudspeakers in each side of a two-port or next to a termination and calculating the so-called "Moore–Penrose pseudoinverse" matrix of either p^+ and p^- we can in fact suppress the flow induced noise inside the duct. Of course it is still required that at least $2N+1$ measurements are linearly independent.

4 Installation

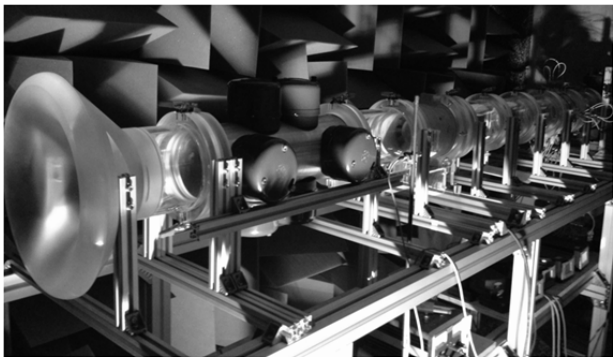

Figure 6: Installation used at VKI, Belgium [7]

The test installation followed the basics of modal decomposition in duct acoustics: two Loudspeaker sets provide for two external sources on each side of the two-port source and two microphone are included to measure their respective sound field. On both duct ends two devices were installed: downstream a prototype version of an inverted anechoic termination [8] and upstream a horn-shaped inlet (see fig. installation). The termination, whose concept is based on the damping of different frequencies in one of its mufflers, was also subjected to tests in order to evaluate its reflective performance. The inlet, located upstream, was positioned in front of the anechoic chamber's flow inlet to minimize non-axial disturbances in the in-duct flow.

The duct intercepted a wall which divided the anechoic chamber. In-duct flow was induced by decreasing pressure on the left mid-chamber.

5 Results

The upstream inlet displayed symmetrical reflection patterns ($R_{N,N_R} = R_{N_R,N}$), which would be related to its axissymetrical shape. Direct reflection coefficients were higher than their convertive counterparts and it was shown how reflection is in general mirrored in the absence of flow. By "mirrored" it's meant that azimuthal modes with opposite azimuthal mode numbers ($m = +N$ and $m = -N$) reflect as each other in equal parts, showing the reflection matrix diagonal to be symmetrical around its center term (plane wave direct reflection coefficient). This symmetry effect constitutes the validation of what had already been suggested in the author's previous work [5].

In-duct flow induced convertive reflections at the same time it lowered direct reflection coefficients both for the anechoic termination and the upstream flow inlet. This effect can be seen as a damping in sound pressure by the presence of flow disturbances.

By testing the reflections at different flow speeds it was possible to observe how increasing the flow speed favors convertive reflection over direct reflection. Both direct and convertive reflection coefficients remained lower for the inlet even when higher flow speeds were used. This meaning the counter reflection effects displayed by the flow could not be overcome by an increase in the flow speeed.

The first radial mode terms decreased as flow assumed higher velocities, retaining lower coefficients for the inlet than for the outlet. These effects were more consistent than those observed for the azimuthal modes which proved more complex to analyze.

For the diaphragm's passive part symmetry was already expected since both sides of the diaphragm are identical. This suggests therefore that in the absence of flow reflection and transmission would process in the same way on both sides. Transmission values were shown to be close to 1 for lower frequencies in accordance to what had already been suggested before by Sack [9].

When a flow speed of 10 m/s (M=0.0294) was induced reflection coefficients on the upstream side were severely increased. Again it was observed how flow having the same direction as reflected waves did not increase reflection significantly, with the upstream side displaying values for direct reflection terms as high as 0.9. The flow did not increase convertive reflections for the upstream side the same way it increased their downstream counterparts. This therefore allows one to understand how flow across a two-port increases direct reflections upstream and convertive reflections downstream. At the same time it suppresses direct reflections downstream, probably due to turbulence effects which make direct reflections less likely to happen.

One should also note that the presence of flow moving in the reflected wave direction is not necessarily a reason why reflection coefficients should increase: sound would move faster in the two-port referential but that does not mean the two-port is more reflective.

Reflection is equally affected by flow, with reflection coefficients being lower downstream (as has already been observed before) both for direct and convertive reflection coefficients alike.

Regarding the ECS fan, passive part tests showed the plane wave transmission coefficient to be higher upstream. This is understandable if previous results for the diaphragm passive part are taken into account, and is expected to be related to sound being carried through the fan by the in-duct flow.

The direct transmission coefficient for the positive first azimuthal mode was significantly higher upstream than downstream. Considering this mode to be a spinning mode it can be understood that a rotation fan induces a flow favorable to the propagation of a first azimuthal mode spinning in the same direction. This effect had already been suggested by Selamt and Ji [10].

At higher frequencies, when higher order modes were included, convertive transmission terms were equally higher for the upstream section, following what had already been referred. The direct transmission coefficient for the first radial mode proved to be three times higher for the upstream section than its downstream counterpart.

Reflection coefficients were overall lower for both sides when the ECS fan was operating. Although not exempt of the lower reflection coefficients for the downstream side, is punctuated by lower reflection values for positive azimuthal modes on the downstream side. This sort of asymmetry is concordant with the theory of "favored spinning directions" already suggested here.

6 Conclusions

The anechoic termination proved to yield higher coefficients for most of reflection terms, not inducing lower values for convertive reflection coefficients. The basic concept of a set of inverted mufflers proved therefore not to suppress reflection as expected, being "less anechoic" then the conventional horn-shaped termination located on the upstream end of the duct.

Research has therefore shown that adding in-duct flow does not increase reflection, rather decreasing direct reflections (most likely due to turbulence effects) and benefiting convertive reflections both when flow has the same direction as the emitted or reflected waves.

In diaphragm tests convertive terms were higher for the downstream side for lower frequencies, assuming then lower values when the frequency and higher order modes were included. This allows us to conclude then that the presence of flow in a ducted diaphragm increases its upstream direct transmission coefficients and lower their downstream counterparts at the same time it favors downstream convertive transmissions while upstream convertive transmission coefficients remain low.

The passive part of an operating ducted fan can therefore be understood as that of a ducted obstacle in the presence of flow which, by inducing rotating speed in the flow, will favor transmission terms for this direction upstream and suppress its reflection counterparts downstream.

The way how transmission and reflection coefficients deviate from their theoretical values when higher order modes are included is evidence of how at cut-on regions the sound field is impossible to describe accurately with the current methodology. Acoustic propagation at these thresholds is complex and still mostly unknown. Cut-on frequencies are interpreted as "transition regions" where modes appear to be hard to identify accurately.

References

[1] M. Åbom, J. Lavrentjev *Characterization of fluid machines a acoustics multi-port sources*. Journal of Sound and Vibration vol. 197, no. 1, pp. 1-16 1996.

[2] S. Rienstra, A. Hirschberg *An Introduction to Acoustics*. Lecture Series Eindhoven University of Technology 2013.

[3] H. Bodén, M. Åbom *Error Analysis of two-microphone measurements in ducts with flow*. Journal of the Acoustical Society of America vol. 83 June 1988.

[4] J. Lavrentjev, M. Åbom, H. Bodén *A measurement method for determining the source data of acoustic two-port sources*. Journal of Sound and Vibration vol. 183, no. 3, pp. 517-531 1995.

[5] J. Aguiar *Mode scattering in ducted fans*. tech. rep. von Karman Institute for Fluyd Dynamics September 2013

[6] S. Allam, H. Bodén, M. Åbom *Over-determination in acoustic two-port data measurement*. ICSV13 - Vienna, The Thirteenth International Congress on Sound and Vibration July 2006

[7] K. Kucukcoskun, J. Aguiar, C. Schram, S. Sack *Aerodynamic and aeroacoustic installation effects in environmental control systems*. ECOMAS, Barcelona, Spain July 2014

[8] bs EN ISO 5136:1999 acoustics *Determination of sound power radiated into a duct by fans and other air-moving devices. in-duct method.* April 2010

[9] S. Sack, M. Åbom, C. Schram, K. Kucukcoskun *Generation and scattering of acoustic modes in ducts with flow*. 20th AIAA/CEAS Aeroacoustics conference June 2014

[10] A. Selamt, Z. L. Ji *Wave reflection from duct terminations*. Journal of the Acoustical Society of America vol. 109, no. 4 April 2001

[11] G. J. Bennett, C. J. O'Reilly, H. Liu *Modelling multi-modal sound transmission from point sources in ducts with flow using a wave-based method*. The Sixteenth International Congress on Sound and Vibration Kraków July 2009